Int J Clin Exp Med 2017;10(2):2241-2251
www.ijcem.com /ISSN:1940-5901/IJCEM0042143

Original Article

Transcript expression profiles of stria vascularis in Mitf-m knockout mice

Wei Chen[1*], Xi Shi[2*], Lili Ren[1], Keshuang Wang[1], Xiaojie Liang[3], Lei Chen[4], Wei Sun[5], Weiwei Guo[1], Shiming Yang[1]

[1]*Department of Otolayngology, Head & Neck Surgery, Institute of Otolaryngology of PLA, Chinese PLA General Hospital, Beijing 100853, China;* [2]*Xuzhou Medical College listening Center, Xuzhou 221006, China;* [3]*Department of Otolaryngeal-Head Neck Surgery, The Army General Hospital of PLA, Beijing 100700, China;* [4]*Key Laboratory of Pig Industry Sciences (Ministry of Agriculture), Chongqing Academy of Animal Science, Chongqing 402460, China;* [5]*Department of Communicative Disorders & Sciences, Center for Hearing and Deafness, State University of New York at Buffalo, Buffalo, New York, United States.* [*]*Equal contributors.*

Received October 17, 2015; Accepted November 15, 2015; Epub February 15, 2017; Published February 28, 2017

Abstract: Objective: Mitf-m gene plays an important role in the development of cochlear stria vascularies. The mutation of Mitf-m gene can cause severe hearing loss, such as Wanderburg syndrome. However, the gene expression change caused by Mitf-m has not been systemically studied. In this paper, we studied the transcriptome of Mitf-m knockout mouse on cochlear stria vascularies. Methods: Total *RNA* extracted from the stria vascularies of the *Mitf-m* knockout mice (*Mitf*$^{mi\text{-}\Delta M/mi\text{-}\Delta M}$, MM group) and the wild type mice (*Mitf-m*$^{+/+}$, WW group) were used for RNA-Seq analysis. The clean reads were mapped to the reference sequence and cufflinks were used to evaluate the RNA sequencing results and gene expression. The program edgeR and DESeq were applied to identify the differentially expressed genes (DEGs). The down-regulated DEGs were further analyzed. Results: A total of 42,463,888 and 39,718,542 clean reads have been mapped to the reference sequence in the MM group and the WW group, respectively. For screening DEGs, 88.7% and 87.4% of the reads were uniquely mapped to the reference sequence suggesting a confidence of the RNA-Seq result. Out of the 45 DEGs, 7 genes were found to be up-regulated and 38 genes were down-regulated. GO enrichment analysis indicated that the down-regulated genes were mainly enriched in pigmentation, the melanin biosynthetic and metabolic process. In addition, these DEGs were involved with the inward rectifier potassium channel activity (*Kcnj10* and *Kcnj13*). KEGG enrichment analysis showed that the down-regulated DEGs mainly enriched in melanogenesis pathways. Conclusion: Our data provide a large amount of useful information about mRNAs that are related in Mitf-m related pathways. The result will help researchers to further understand the functions of Mitf-m as a master regulator in more pathways, such as cell proliferation, DNA repair, cell cycle, apoptosis, proliferation, malanosome, and Na^+/K^+ iron pathway. Together, our data provide a novel insight for Mitf-m network function.

Keywords: *Mitf-m,* stria vascularis, RNA sequencing, knockout mice

Introduction

According to recent estimates of the World Health Organization (WHO), more than 5% of the world's total population suffered from some form of disabling hearing loss (WHO, 2014). It was found that abnormal pigmentation and hearing loss were frequently combined in most mammals. In human, Waardenburg syndrome (WS) is characterized by varying combinations of sensorineural hearing loss, heterochromia iridis and patchy abnormal depigmentation of the hair and skin [1]. WS is clinically and genetically heterogeneous and classified into four types (WS 1, WS 2, WS 3 and WS 4). WS 1 and WS 3 are caused by loss of function mutation in the PAX3 gene, while mutation in EDNRB, EDN3 and SOX10 can be the cause of WS 4 [2]. Among those subtypes of WS, WS 2 is a dominantly inherited disorder and is associated with mutation in the microphthalmia-associated transcription factor (Mitf) gene [3]. Mitf is a tissue restricted, basic helix-loop-helix leucine zipper (b-HLH-Zip), and dimeric transcription factor. Mitf plays a critical role in the development of both neural-crest-derived melanocytes and optic cup-derived retinal pigmented epithelium (RPE); the loss of a functional Mitf in mice results in complete absence of all pigment cells, which in turn induces microphthalmia and

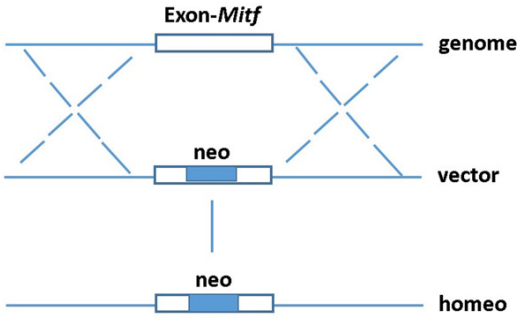

Figure 1. Schematics show the process of *Mitf-m* targeting. Top: The region of the *Mitf* gene containing exon m, exon 2, exon 3, and exon 4; Middle: The targeting construct with a floxed neomycin cassette in the Mpromoter/Mexon region; Bottom: *Mitf* gene portion after targeting.

inner ear deafness [4]. Mitf is also a melanocyte master regulator gene and a melanoma oncogene [5]. The Mitf gene contains multiple promoters and consecutive first exons, followed by common downstream exons, thereby generating distinct isoforms that differ in theamino-termini, such as Mitf-M, Mitf-A, Mitf-D and Mitf-H [6].

In 1957, Kreinter reported a recessive white spotting mutation that was subsequently termed black-eyed white ($Mitf^{mi\text{-}bw}$) [7]. The mouse homozygous for the Mitf mi-bw allele shows a complete black-eyed white phenotype with severe hearing loss but without apparent ocular abnormalities [4, 8]. It was found that the 7.2 Kb L1 element was inserted into intron 3 that specifically repress the transcription from the melanocyte-specific promoter and lead to the decreased expression of Mitf-m mRNA [4]. Although Mitf mi-bw provided a good model to study the function of Mift-m, the 7.2 kb L1 element insertion within intron 3 is spontaneous and there is possible affect on the transcription of other type of Mift.

In the present study, we investigated the different expression of mRNAs in transgenic Mitf-gene using RNA-seq technology. We used transcriptome sequencing technology to analyses and identify the full repertoire of mRNAs expressed in the Mitf pathways. The data provide a large amount of useful information about mRNAs that are associated to Mitf related pathways. The result will help researchers to further understand the functions of Mitf as a master regulator in more pathways, such as cell proliferation, DNA repair, cell cycle, apoptosis, proliferation, malanosome, and Na^+/K^+ iron pathway. Together, our data provide a novel insight for Mitf network function.

Materials and methods

Mice

$Mitf^{mi\text{-}\Delta M/mi\text{-}\Delta M}$ targeted mice were generated using the recombineering technology. To generate the targeting construct, the M-promoter/M-exon and its flanking regions (10,868 bp) were cloned using plasmid rescued from BACRP23-9A13. A 1,743 bp floxed neomycin resistance expression cassette, which was flanked by 160 bp of sequence flanking the M-promoter/M-exon, was used to replace 790 bp of the M-promoter/M-exon from the above plasmid (**Figure 1**). The targeting construct was used for standard targeting of CRIB 6.1 ES cells (genotype [C57Bl6J/6Nx129S6] F1), giving 6 correctly targeted colonies out of 40 colonies tested. Positive ES cell clones were micro injected into 8-cell embryos to obtain chimeric mice. The Chimeric mice that transmitted the modified Mitf M-exon allele to their progeny were crossed with Kunming mice to generate $Mitf^{mi\text{-}\Delta M/+}$ mice. $Mitf^{mi\text{-}\Delta M/mi\text{-}\Delta M}$ targeted mice were obtained by $Mitf^{mi\text{-}\Delta M/+} \times Mitf^{mi\text{-}\Delta M/+}$ mating. Genotyping of mice was performed by PCR using primers which flanking M-exon of Mitf shown in Supplementary Table 1. The use of mice has been approved by the Institutional Animal Care and Use Committee of the General Hospital of PLA in Beijing.

Dissection of mouse stria vascularis

Heads of anesthetized animals were cut down after the auricle with a guillotine. The heads were split along the middle line to remove the brain tissues. The bilateral otic vesicle was dissociated carefully using the rongeur. The bone shell of the otic vesicle was opened to expose the cochlear structures. The dissected cochlea was put into the glass dish that filled with RNA later solution (Life Technologies, Carlsbad, CA). The cochlea volute was quickly removed under the dissection microscope and the stria vascular was removed from the outer wall of the cochlea by the gossamer tweezers. The Reissner's membrane was to from the edge of the stria vascular to get the complete stria vasculars.

RNA extraction

Total RNA of stria vascularis was isolated by a TRIzol Plus RNA Purification Kit (Life

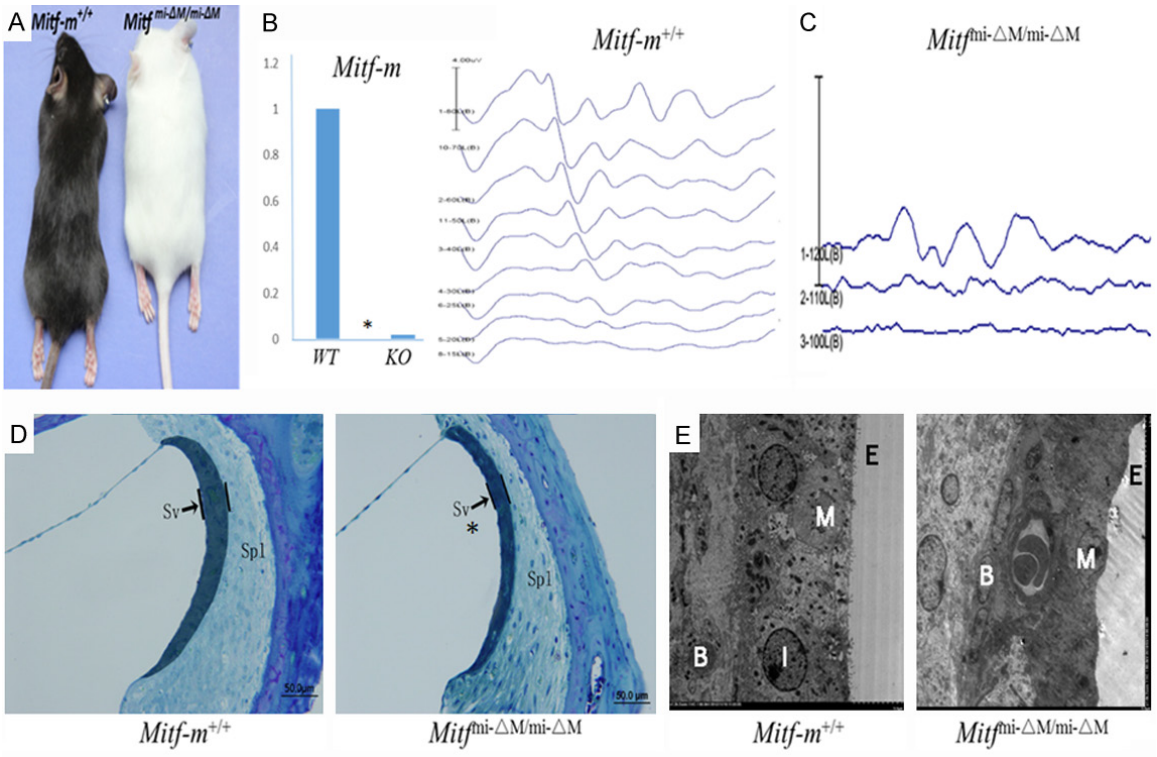

Figure 2. The phenotype of *Mitfm* knockout mice. A. *Mitf*$^{+/+}$ shows black coat color, and *Mitf* $^{miΔM/miΔM}$ shows white coat color and black eyes. B. *Mitf-m* was not detected in *Mitf* $^{miΔM/miΔM}$ cochlea, but expressed in *Mitf*$^{+/+}$ cochlea. C. The ABR threshold are 20~30 dB SPL in *Mitf*$^{+/+}$ mice, and 100~110 dB SPL in *Mitf* $^{miΔM/miΔM}$ mice. D. The stria vascularis (SV) of *Mitf* $^{miΔM/miΔM}$ cochlea are significantly thinner and shorter than that of *Mitf*$^{+/+}$ as indicated by stars. E. The image of transmission electron microscope (TEM) showing most of the melanocytes were abnormal or missing in the cochlea of *Mitf* $^{miΔM/miΔM}$.

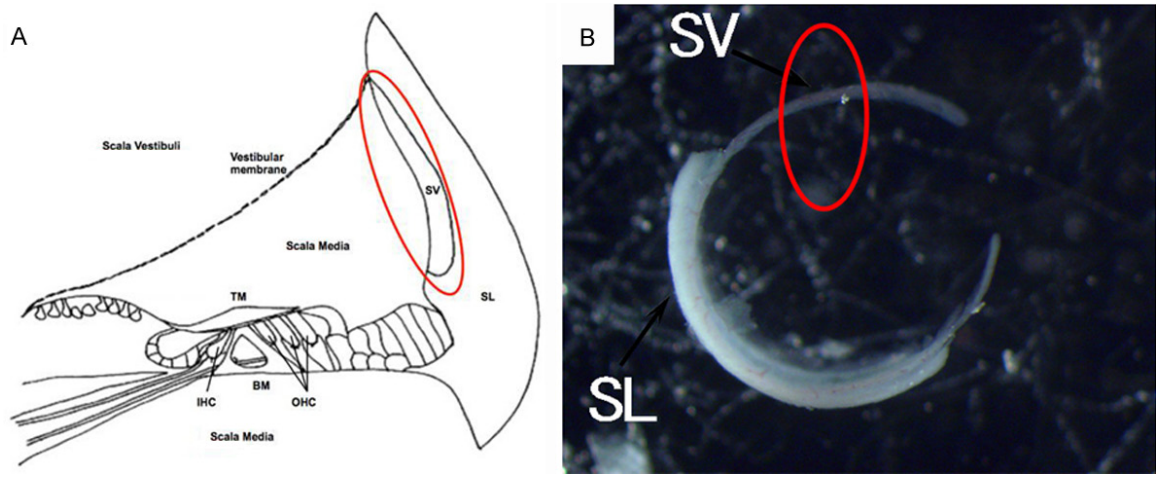

Figure 3. Dissection of mouse stria vascularis (SV) for RNA-seq. The schematic cross-section (A) and photograph (B) show the dissection protocol. Firstly, the organ of Corti and lateral wall were peeled away from the spiral ganglion, the lateral wall was peeled away from the organ of Corti. The fraction of lateral wall contains the spiral ligament, outer sulcus, and stria vascularis. Then, the cochlear outer wall and the Reissner's membrane was removed to get the complete tissue of stria vascularis.

Technologies, Carlsbad, CA) and RNase-free DNase I was used to eliminate the residual genomic DNA in the raw RNA extract, according to the manufacturer's protocol (Promega, Beijing, China) with minor revisions. The concentration and quality of total RNA were deter-

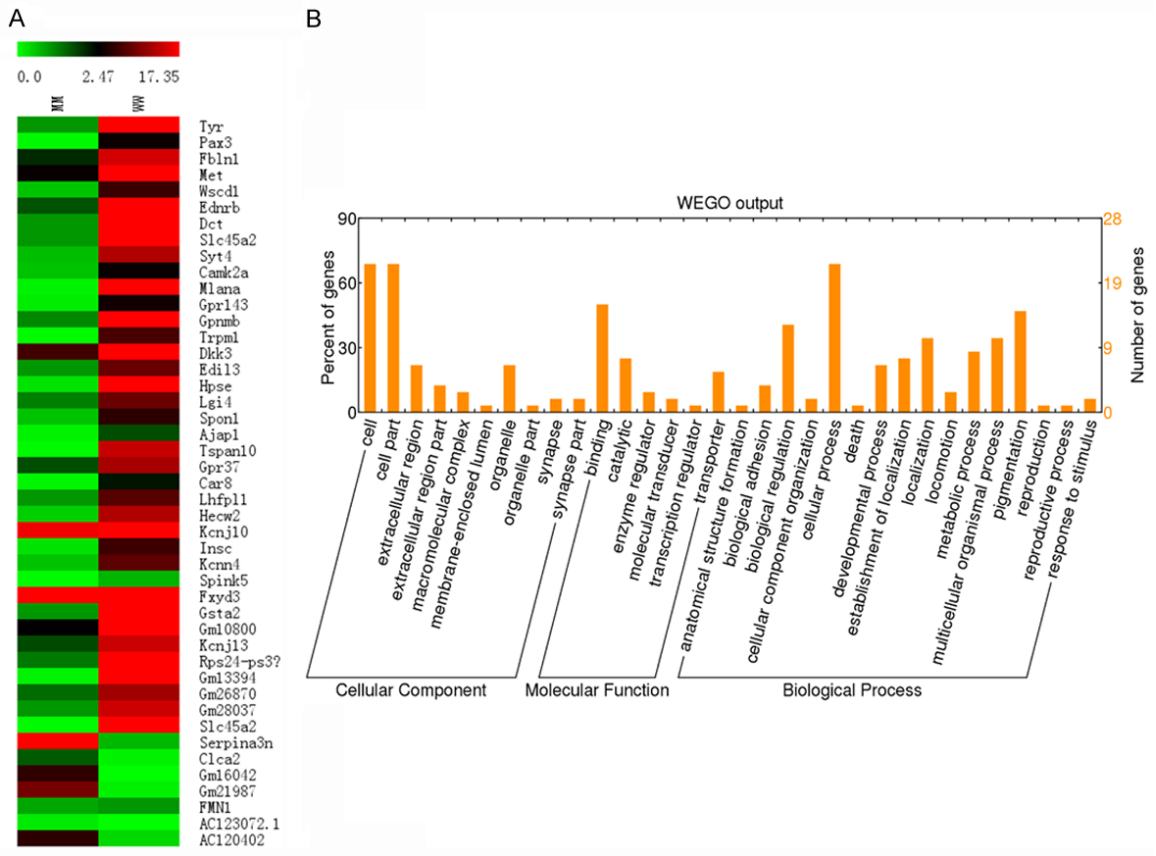

Figure 4. Heat-map view of differentially expressed genes (DEGs) (A) and Gene Ontology classification of the transcriptome (B). (A) Each column represents an experimental sample, and each row represents a gene. Expression differences are shown in different colors. Red indicates high expression and green indicates low expression. (B) Histogram of the GO annotation was generated by KOBAS (kobas.cbi.pku.edu.cn). The unigenes were grouped into three main GO categories: cellular component, molecular function and biological process. The right Y-axis indicates the number of unigenes in a category. The left Y-axis indicates the percentage of a specific category. One unigene could be assigned with more than one GO term.

mined by spectrophotometer analysis and using denaturing agarose gel electrophoresis.

Expression analysis

The mRNA expression levels of Mitf transcriptional variants and β--actin were analyzed by a qPCR method using the primers in Supplementary Table 1. The cDNA samples (100 ng) and primers for the target genes were mixed with Power SYBR Green PCR Master Mix (Life Technologies, Carlsbad, CA) in 25 μL final volumes, and amplified using an ABI 7900 instrument (Life Technologies, Carlsbad, CA). All samples were analyzed in triplicate. Protein expression levels of Mitf isoforms and tubulin were examined by immunoblotting assays using lysed tissue from Mitf R/R and Mitf r/r cochleae.

The cDNA library preparation and Illumina sequencing for transcriptome analysis

According to the Illumina manufacturer's instructions, poly (A)+ RNA was purified from 20 μg of total RNA of three wildtype and three targeted mice using oligo (dT) magnetic beads and fragmented into short sequences in the presence of divalent cations at 94°C for 5 min. Next, the first strand of cDNA was synthesized by using a random hexamer primer. Buffer, dNTPs, RNAase H, and DNA polymerase I were added to synthesize the second strand. After the end repair and ligation of adaptors, the products were amplified by PCR and purified using the PureLink PCR Purification Kit (Invitrogen) to create a cDNA library. The fragments were enriched by polymerase chain reaction (PCR) amplification and purified to cre-

Table 1. Differential genes in MM group compared to WW group

A. Down-expression genes

Id	Gene Name	MM_FPKM	WW_FPKM	Log Fold Change	*P* value	FDR *P* value
ENSMUSG00000004651	Tyr	0.00	37.48	13.98	5.66E-22	2.90E-18
ENSMUSG00000004872	Pax3	0.05	3.29	6.18	2.36E-10	3.71E-07
ENSMUSG00000006369	Fbln1	2.07	14.95	2.81	8.56E-05	3.58E-02
ENSMUSG00000009376	Met	3.03	37.39	3.73	3.33E-07	3.10E-04
ENSMUSG00000020811	Wscd1	0.58	5.96	3.36	8.90E-06	5.52E-03
ENSMUSG00000022122	Ednrb	1.66	26.91	4.01	8.27E-08	8.47E-05
ENSMUSG00000022129	Dct	0.00	774.43	18. 09	2.46E-34	5.03E-30
ENSMUSG00000022243	Slc45a2	0.00	45.18	14.05	3.31E-22	2.26E-18
ENSMUSG00000024261	Syt4	0.63	12.83	4.39	1.35E-08	1.63E-05
ENSMUSG00000024617	Camk2a	0.58	3.10	2.89	9.61E-05	3.94E-02
ENSMUSG00000024806	Mlana	0.11	90.85	9.38	1.06E-16	3.09E-13
ENSMUSG00000025333	Gpr143	0.17	3.58	4.15	1.09E-05	6.21E-03
ENSMUSG00000029816	Gpnmb	1.15	86.55	6.24	4.48E-14	1.15E-10
ENSMUSG00000030523	Trpm1	0.04	6.76	7.09	6.11E-12	1.14E-08
ENSMUSG00000030772	Dkk3	6.46	88.21	3.78	2.34E-07	2.28E-04
ENSMUSG00000034488	Edil3	1.00	8.71	3.18	1.24E-05	6.52E-03
ENSMUSG00000035273	Hpse	0.28	168.19	9.42	2.22E-22	2.26E-18
ENSMUSG00000036560	Lgi4	1.23	8.81	3.55	3.88E-06	2.74E-03
ENSMUSG00000038156	Spon1	0.58	5.12	3.14	1.63E-05	8.37E-03
ENSMUSG00000039546	Ajap1	0.12	1.73	4.30	4.90E-06	3.34E-03
ENSMUSG00000039691	Tspan10	0.04	14.14	8.33	1.26E-13	2.87E-10
ENSMUSG00000039904	Gpr37	1.71	12.30	2.86	6.24E-05	2.72E-02
ENSMUSG00000041261	Car8	0.08	2.27	4.81	6.17E-08	6.65E-05
ENSMUSG00000041700	Lhfpl1	0.00	7.66	10.32	2.72E-11	4.64E-08
ENSMUSG00000042807	Hecw2	0.46	12.81	3.34	5.76E-06	3.68E-03
ENSMUSG00000044708	Kcnj10	16.59	111.93	2.77	7.17E-05	3.06E-02
ENSMUSG00000048782	Insc	0.27	6.08	4.22	4.38E-07	3.90E-04
ENSMUSG00000054342	Kcnn4	0.58	7.91	3.76	1.72E-06	1.41E-03
ENSMUSG00000055561	Spink5	0.04	0.70	3.99	1.22E-05	6.52E-03
ENSMUSG00000057092	Fxyd3	17.35	99.84	2.85	5.62E-05	2.50E-02
ENSMUSG00000057933	Gsta2	0.00	26.24	10.97	3.85E-13	7.89E-10
ENSMUSG00000075014	Gm10800	2.67	39.97	3.94	2.18E-06	1.72E-03
ENSMUSG00000079436	Kcnj13	1.75	14.40	3.04	4.66E-05	2.12E-02
ENSMUSG00000081049	Rps24-ps3	1.29	20.59	3.88	2.18E-05	1.09E-02
ENSMUSG00000083773	Gm13394	0.11	71.28	9.09	9.04E-18	3.70E-14
ENSMUSG00000097312	Gm26870	1.42	11.92	3.06	3.48E-05	1.66E-02
ENSMUSG00000098371	Gm28037	0.00	14.45	9.80	6.94E-10	8.88E-07
ENSMUSG00000102823	Slc45a2	0.04	31.19	9.43	7.66E-17	2.61E-13

B. Up-expression genes

Id	Gene Name	MM_FPKM	WW_FPKM	logFold Change	*P* value	FDR *P* value
ENSMUSG00000021091	Serpina3n	22.07	0.68	-4.96	5.75E-10	7.85E-07
ENSMUSG00000028262	Clca2	1.59	0.12	-3.77	9.52E-06	5.73E-03
ENSMUSG00000090407	Gm16042	5.28	0.01	-9.92	3.22E-10	4.71E-07
ENSMUSG00000095464	Gm21987	9.36	0.13	-5.58	2.47E-06	1.80E-03
ENSMUSG00000100934	FMN1	0.85	0.00	-9.23	2.04E-08	2.33E-05
ENSMUSG00000103888	AC123072.1	0.19	0.01	-4.68	5.64E-07	4.81E-04
ENSMUSG00000104049	AC120402	5.12	0.37	-3.77	5.58E-06	3.68E-03

Genes that increased more than 2.0-fold were selected and ordered based on fold change values. $^{*}P<0.05$, $^{**}P<0.001$, significantly different from the wild type.

Table 2. Differential genes enrichment GO-Terms

GO-Term	GO ID	Input number	Background Number	*P* value	Corrected *P*-Value
Pigmentation	GO:0043473	6	76	1.37E-08	1.68E-05
Developmental pigmentation	GO:0048066	4	44	2.28E-06	0.001398
Melanin biosynthetic process	GO:0042438	3	14	4.44E-06	0.001548
Melanin metabolic process	GO:0006582	3	15	5.32E-06	0.001548
Secondary metabolite biosynthetic process	GO:0044550	3	16	6.30E-06	0.001548
Melanosome	GO:0042470	3	22	1.48E-05	0.002603
Pigment granule	GO:0048770	3	22	1.48E-05	0.002603
Phenol-containing compound biosynthetic process	GO:0046189	3	33	4.53E-05	0.006961
Secondary metabolic process	GO:0019748	3	36	5.78E-05	0.007886
Pigment biosynthetic process	GO:0046148	3	39	7.23E-05	0.008878
Pigment metabolic process	GO:0042440	3	49	0.000137	0.015321
Organic hydroxy compound biosynthetic process	GO:1901617	4	164	0.000313	0.029588
Inward rectifier potassium channel activity	GO:0005242	2	14	0.000417	0.036601
Phenol-containing compound metabolic process	GO:0018958	3	80	0.000546	0.044724

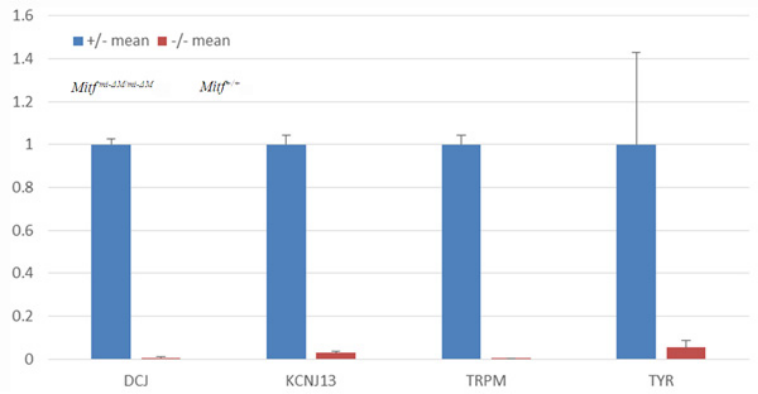

Figure 5. The four down regulated genes were validated by qPCR.

ate cDNA libraries. The Agilent 2100 Bioanalyzer and the ABI Step One Plus Real-Time PCR System were used respectively to quantify and qualify the sample libraries. Finally, the cDNA libraries were sequenced using HiSeq 2000 Sequencing System (Illumina, Inc., USA). De novo assembly, function annotation and classification were started after removing the reads contained adaptor contamination. Transcriptome de novo assembly was carried out with the short-read assembly program Tophat 2.2.0 (http://ccb.jhu.edu/software/tophat/index.shtml) [9]. The resulting sequences were considered unigenes. The removal of redundant sequences and further splicing of the assembled unigenes from each sample were carried out using the software program RSeQC-2.3.2 (http://code.google.com/p/rseqc/) [10], after which sequence clustering software was used to acquire non-redundant unigenes for as long as possible. BLASTX alignments (E-value < 10e-5) between unigenes and protein databases, including Ensembl, the Kyoto Encyclopedia of Genes and Gezznomes (KEGG), and COG, were performed, and the best aligned results were used to determine the sequence direction of unigenes. The program of edgeR (http://bioconductor.org/packages/release/bioc/html/edgeR.html) [11] and DESeq (http://bioconductor.org/packages/release/bioc/html/DESeq.html) [12] were used to annotate the differential genes.

Statistics

The normally distributed continuous variables were showed as mean ± SD (standard deviation). Between groups, t-test or ANOVA was used to analyze and compare quantitative data. The data abnormally distributed were analyzed between groups with Kruskal-Wallis ANOVA method. SPSS software (version 18.0) was used to analyze these statistical data, with $P < 0.05$ considered statistically significant.

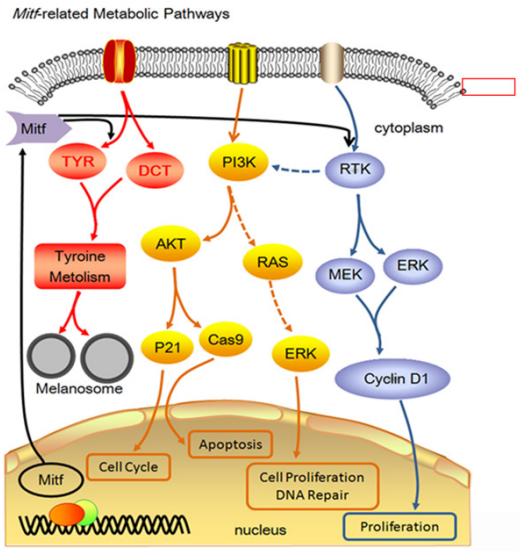

Figure 6. *Mitf*-related metabolic pathways identified by KEGG annotation. The red box indicates that the genes identified in our research are annotated in the metabolic pathways and the green genes names were all taken part in this pathways.

Results

Mitf-m specific mutations result in hearing loss in a mouse model

To generate Mitf-M targeted mice, 790 bp of the M-promoter/M-exon was replaced by a neomycin cassette (**Figure 1**). Mitf$^{mi\text{-}\Delta M/mi\text{-}\Delta M}$ mice displayed profound hypopigmentation, with white hair and skin in contrast to the black coat of wild type (**Figure 2A**). A quantitative PCR assay confirmed that the expression of Mitf-m was detected in Mitf$^{mi\text{-}\Delta M/mi\text{-}\Delta M}$ cochlea (**Figure 2B**). ABR tests revealed profound hearing loss in Mitf$^{mi\text{-}\Delta M/mi\text{-}\Delta M}$ mice (**Figure 2C**). Interestingly, the cochlear striavascularis (SV) of targeted mice were markedly thinner observed by blood vessel slices (**Figure 2D**), and the image of scanning electron microscopy (SEM) showed that there were no intermediate melanocyte cells in the Mitf$^{mi\text{-}\Delta M/mi\text{-}\Delta M}$ mice (**Figure 2E**). In our previous study, loss of hair cells and stereocilia bundles in the cochleae of Mitf$^{mi\text{-}\Delta M/mi\text{-}\Delta M}$ mice was also observed by SEM [13]. These results are similar with the WS2 patients within hearing loss that is known to be caused by a deformed [14].

Transcriptomic analysis of Mitf$^{mi\text{-}\Delta M/mi\text{-}\Delta M}$ mices-triavascularis

To investigate the role of Mitf-M in mice stria vascularis, two libraries were generated for RNA-seq. We developed a two steps method to dissect the SV from mouse (**Figure 3**). First, the head was cut down with a guillotine, then the auricle was splited along the middle line and brain tissues were removed. Carefully use the rongeur, the bilateral otic vesicle was dissociated, and then the bone shell of the otic vesicle was opened, the cochlear structure was exposed. Second, dissected cochlea were put into the glass dish which was filled with RNA later solution. Under the dissection microscope, quickly remove the cochlea volute and carefully use the gossamer tweezers to remove the stria vascular from the outer wall of the cochlea, then tear the Reissner's membrane from the edge of the stria vascular, complete stria vasculars were then subjected to cDNA library preparation and sequenced in parallel using an Illumina HiSeq. In this study, MM is the stria vascular from Mitf$^{mi\text{-}\Delta M/mi\text{-}\Delta M}$ mice and WW is the counter part of wildtype mice of the same litter to provide the same genetic background. Each library produced about 45M clean read. More than 91% percent of clean reads were mapped to mouse genome by Tophat assembly program. These data showed enough throughputs and sequencing quality for further gene expression analysis.

Two methods were used to analyze the differentially expressed genes named edgeR and DEseq. The edgeR program produced 51 DEGs and DESeq produced 191 DEGs. There are 45 DEGs predicted by both edgeR and DEseq (**Figure 4A**). Of the 45 overlap DEGs, 7 genes are up-regulated and 38 genes are down-regulated (**Table 1**). The proportions and comparisons between up-regulated and down-regulated genes were summarized in three main functional categories (**Figure 4B**) and the DEGs enriched GO-term were listed in **Table 2**. The pigmentation metabolic and biosynthetic processes were major responsive classes. This suggests that metabolic processes are reduced.

Mitf-M regulated Kir channel through Kcnj13 and Kcnj10

The endolymphatic space contains luminal fluid with high potassium concentration ([K^+]) and low sodium concentration ([Na^+]), which provides the ionic milieu needed to sustain transduction of sound and head acceleration into nerve impulses necessary for normal hearing and balance. Kir channels were important for

the K^+ cycling. K^+-transport channels were one of the four sub-groups of Kir channels. *Kcnj10*, potassium inwardly-rectifying channel, subfamily J, member 10 encodes Kir 4.1 channel and *Kcnj13*, potassium inwardly-rectifying channel, subfamily J, member 13 encoded Kir 7.1. Both *Kcnj10* and *Kcnj13* were down-regulated in the stria vascularis of $Mitf^{mi\text{-}\Delta M/mi\text{-}\Delta M}$ mice (**Figure 5**). We were able to confirm the down regulated gene expression in the stria vascularis of $Mitf^{mi\text{-}\Delta M/mi\text{-}\Delta M}$ mice by qPCR.

Mitf-M play important role in melanogenesis pathway

To evaluate the validity of RNA-seq analysis, four differential genes including *Dcj, Kcng13, Tyr* and *Trpm1*related to melanogenesis pathway were further selected to be examined by real-time RT-PCR. The RNA-seq results of these genes were identical to those obtained by quantitative PCR. We found that gene expression profiling of these DEGs using qPCR revealed similar variation trends with RNA-Seq samples, which indicated the high credibility of difference in these genes at transcript level between MM and WW. To provide a global view of Mitf-related metabolic pathways, DEGs were subjected by KEGG annotation (**Figure 6**). *Dct* and *Tyr* were proved to be important in the melanogenesis pathway.

Discussion

Mutations in the M (melanocytic) isoform of Mitf are known to lead to Waardenburg syndrome type 2A (MIM 193510), an autosomal dominant disorder characterized by variable degrees of sensorineural hearing loss and pigmentation disorders of the skin, skin appendages and irides [1]. Dysfunction in melanocytes in the SV is the major pathology of WS 2. Apart from MitfM, isoforms MitfA and Mitf-H are also expressed in melanocytes and melanoma cells. Thus, the function of each isoform in hearing loss cannot be identified exclusively. In a previous study of $Mitf^{mi\text{-}bw}$ mice, insertion of a retrotransposing L1 element into intron 3 of the Mitf gene abolished MitfM, but also affected the expression of MitfA and MitfH [4]. Thus, the phenotypes on hearing loss and pigmentation cannot be imputed exclusively to the elimination of MitfM. In this study, Mitf-m targeted mice were generated by insert 790 bp neomycin cassette within the M-promoter/M-exon (**Figure 1**). $Mitf^{mi\text{-}\Delta M/mi\text{-}\Delta M}$ displayed profound hypopigmentation and hearing loss (**Figure 2**). This phenotype is similar to that of $Mitf^{mi\text{-}bw}$ mice [4]. To validate the specific of $Mitf^{mi\text{-}\Delta M/mi\text{-}\Delta M}$ expression of Mitf-A, Mitf-H, Mitf-J and Mitf-M in the cochlea, there expressions were detected. There were no obvious difference for the expression of Mitf-A and Mitf-H, but interestingly the Mitf-J expression were increased (**Figure 2C**). The Mitf-M might be the repressor of Mift-J. More detailed biological understanding of the impact of this regulation remains to be learned. Take the advantage of MitfM specific targeted $Mitf^{mi\text{-}\Delta M/mi\text{-}\Delta M}$, the SV were dissected for RNA-seq to further investigate the role of MitfM in hearing loss. Here report that 7 genes are up-regulated and 38 genes are down-regulated (**Table 1**).

Serpins (serin peptidase inhibitors or SPIs) are the largest family of protease inhibitors and extend to all branches of life [15]. Members of this class of protein perform roles in diverse physiological processes such as the blood clotting cascade, apoptosis and chromatin condensation [16]. Serpina3n represents the serine (or cysteine) peptidase inhibitor, clade A, member 3N. Up-regulated expression of Serpina3n was reported as a consequence of genetically deleting Tff 3 in mice, indicating a potential role of this factors during the development of presbyacusis [17]. It is worthwhile mentioning that a member of the serpin gene family, SERPINB6, has recently been associated with hearing loss in human patients [18]. Therefore, further studies directed at the function of serpina3n in hearing loss of the Tff 3 knockout mouse model may provide important insights on the roles of these genes during the development of age-related hearing loss.

Calcium activated chloride (CLC) currents have been characterized in a number of cell types including smooth muscle, skeletal muscle and epithelium. Proteins belonging to CLC, CLCA, bestrophin and twenty gene families have been proposed to function as calcium activated chloride channels. The CLCA gene family includes 6 genes in mouse. Clca2 is expressed in mouse brain and cerebral cortex, albeit at very low levels [19]. Our report for the first time describe the expression of Clca2 in mouse SV and was upregulated in Mitf-M mouse. The role of Clca2 in hearing loss is remained to be studies.

The formin family of proteins controls the rate of actin nucleation at its barbed end. Thus,

formins are predicted to contribute to several important cell processes such as locomotion, membrane ruffling, vesicle endocytosis, and stress fiber formation and disassociation [20]. The genomic rearrangements of GREM1-FMN1 locus on chromosome 15q13.3.43 is the genetic cause of Cenani-Lenz phenotype with hearing loss [21]. This is the first report shown that FMN1 might play a role in the hearing loss of the Mitf-M mice. Other four genes including Gm16042, Gm21987, AC123072.1 and AC12-0402 are predicted gene, there function have not been studied yet. The expression of four down-regulated genes was validated by qPCR (**Figure 5**). Interestingly, Kcnj10 and Kcnj13 were down-regulated in the stria vascularis of $Mitf^{mi\text{-}\Delta M/mi\text{-}\Delta M}$ mice.

Kir channels exhibit an asymmetrical conductance at hyperpolarization (high conductance) compared to depolarization (low conductance) and demonstrate an inward rectification in the current-voltage relationship. Kir channel shave a critical role in the inner ear for hearing. Kir4.1is a predominant isoform in the inner ear. Mutations or knockout (KO) of Kir4.1 (Kcnj10) induce hearing loss [22, 23]. Kir4.1 mRNA is the only detectable Kir channels in the SV [24]. In this study, we found that both Kir4.1and kir 7.1 were expressed in SV by RNA-seq and qPCR.

The EP is a driving force for hair cells to produce the auditory receptor current. The positive EP and high concentration of K^+ in the endolymph are generated by the cochlear lateral wall [25]. Kir channels play an essential role in the generation of the EP [26]. In SV of $Mitf^{mi\text{-}\Delta M/mi\text{-}\Delta M}$ mice, both Kir4.1 and Kir7.1 mRNA were reduced significantly, this suggest that Mift-M play an important role in hearing by activating of Kir4.1 and Kir7.1 mRNA in normal EP.

Mitf is a tissue-restricted master regulator of melanocytes, and is essential for their proliferation, survival, and differentiation. Mitf is subject to various post-translational modifications, particularly phosphorylation by mitogen-activated protein kinase (MAPK), ribosomal S6 kinase (RSK), glycogen synthase kinase-3b (GSK3b) and p38 [6]. These kinases reside within various important homeostatic signaling pathways and might therefore modulate Mitf transcriptional activity in response to specific environmental cues. Our RNA-seq result indicated the Mitf is involved in the tyrosine metabolism pathway through DCT/TYR.

An idea popular in the current literature is that signaling pathways, rather than individual genes, are recurrently perturbed in Mitf gene functions [27]. To determine whether the Mitf-genes from different melanoma cell lines shared membership of one or more cellular pathways, we investigated whether the proteins encoded by the Mitf-genes were connected in known human protein interaction networks (for details see Materials and Methods). Following detailed manual annotation, the resulting pathways were ranked according to the number of contributing to the number of Mitf-genes involved in the pathway. Interestingly, the vast majority of the recurrent pathways we identified involve signal transduction. Pathway modules including WNT, melanogenesis and ErbB signaling pathway were common to all published datasets [27].

KCNJ 13, encoding inwardly rectifying potassium channel subunit Kir7.1, is expressed at the apical side of the retinal pigment epithelium (RPE) [2-4]. Kcnj13 appears to act in a non-cell-autonomous manner and indirectly regulates photoreceptor cell survival. A member of the inwardly rectifying potassium (Kir) channel family, Kir7.1 is encoded by KCNJ13, a gene mapped to chromosome 2 at 2q37. Formed by the synchronous- assembly of four Kir7.1subunits, the channel is unique among members of the Kir channel family, in that it has a very low estimated singlechannel conductance of 50-200 nS and a much larger macroscopic conductance to Rb^+ than to K^+ [22, 24, 28]. In the RPE, Kir7.1 channels are localized at the apical surface and microvilli and account for the large K^+ conductance of the apical membrane. From this strategic location, these channels mediate K^+ secretion into the subretinal space, which serves to sustain Na^+/K^+ pump activity, buffer light-evoked decreases in subretinal K^+ concentration, and help determine the direction and magnitude of transepithelial K^+ transport [29]. By establishing a large negative membrane potential, Kir7.1 channels also influence the driving forces and, thus, transport of other ions and solutes via channels and electrogenic transporters (**Figure 6**) [28]. There is no report about the relationship of Kcnj 13 and Mitf. Coupling of MC4R to Kir7.1 may explain unusual aspects of the control of energy homeostasis by melano, cortin signalling, including the gene dosage effect of MC4R and the sustained effects of AgRP on food intake [11].

In summary, we have investigated the differential transcriptome of MitfM specific targeted $Mitf^{mi\text{-}\Delta M/mi\text{-}\Delta M}$. Our data determined 7 up-regulated and 38 down-regulated genes. The down regulated *Kcnj 10* and *Kcnj13* revealed by qPCR suggested the important role of Mitf-M in activating of Kir4.1 and Kir7.1 mRNA transcription in SV. The elucidation of Kir channel regulation by Mift-M in cochlear development.

Acknowledgements

This work was supported by grants from the National Basic Research Program of China (973 Program) (#2012CB967900), and the National Natural Science Foundation of China (No. 81670940, 81570933).

Disclosure of conflict of interest

None.

Address correspondence to: Drs. Shiming Yang and Weiwei Guo, Department of Otolaryngology, Head & Neck Surgery, Institute of Otolaryngology, Chinese PLA General Hospital, Beijing 100853, China. Tel: 86-10-68211696; Fax: 86-10-68211696; E-mail: yangsm301@263.net (SMY); gwent001@163.com (WWG)

References

[1] Read AP, Newton VE. Waardenburg syndrome. J Med Genet 1997; 34: 656-665.

[2] Tamayo, ML, Gelvez N, Rodriguez M, Florez S, Varon C, Medina D, Bernal JE. Screening program for waardenburg syndrome in colombia: clinical definition and phenotypic variability. Am J Med Genet A 2008; 146: 1026-1031.

[3] Tassabehji M, Newton VE, Read AP. Waardenburg syndrome type 2 caused by mutations in the human microphthalmia (mitf) gene. Nat Genet 1994; 8: 251-255.

[4] Yajima I, Sato S, Kimura T, Yasumoto K, Shibahara S, Goding CR, Yamamoto H. An l1 element intronic insertion in the black-eyed white (mitf [mi-bw]) gene: the loss of a single mitf isoform responsible for the pigmentary defect and inner ear deafness. Hum Mol Genet 1999; 8: 1431-1441.

[5] Steingrímsson E, Copeland NG, Jenkins NA. Melanocytes and the microphthalmia transcription factor network. Annu Rev Genet 2004; 38: 365-411.

[6] Levy C, Khaled M, Fisher DE. Mitf: master regulator of melanocyte development and melanoma oncogene. Trends Mol Med 2006; 12: 406-414.

[7] Kreinter PC. Linkage studies in a new black-eyed white mutation. J Hered 1957; 48: 300-304.

[8] Motohashi H, Hozawa K, Oshima T, Takeuchi T, Takasaka T. Dysgenesis of melanocytes and cochlear dysfunction in mutant microphthalmia (mi) mice. Hear Res 1994; 80: 10-20.

[9] Kim D, Pertea G, Trapnell C, Pimentel H, Kelley R, Salzberg SL. Tophat2: accurate alignment of transcriptomes in the presence of insertions, deletions and gene fusions. Genome Biol 2013; 14: 295-311.

[10] Wang L, Wang S, Li W. Rseqc: quality control of rna-seq experiments. Bioinformatics 2012; 28: 2184-2185.

[11] Robinson MD, Mccarthy DJ, Smyth GK. Edger: a bioconductor package for differential expression analysis of digital gene expression data. Bioinformatics 2010; 26: 139-140.

[12] Anders S, Huber W. Differential expression analysis for sequence count data. Genome Biol 2010; 11: 1-12.

[13] Weiwei G, Yongyi Y, Zhaohui H, Xiang W, Shiming Y. Profiles of the auditory epithelia related microRNA expression in neonatal and adult rats. Eur J Med Res 2014; 19: 48.

[14] Steel KP, Barkway C. Another role for melanocytes: their importance for normal stria vascularis development in the mammalian inner ear. Development 1989; 107: 453-463.

[15] Irving JA, Pike RN, Lesk AM, Whisstock JC. Phylogeny of the serpin superfamily: implications of patterns of amino acid conservation for structure and function. Genome Res 2000; 10: 1845-1864.

[16] Silverman GA, Bird PI, Carrell RW, Church FC, Coughlin PB, Gettins PG, Irving JA, Lomas DA, Luke CJ, Moyer RW, Pemberton PA, Remold-O'Donnell E, Salvesen GS, Travis J, Whisstock JC. The serpins are an expanding super family of structurally similar but functionally diverse proteins evolution, mechanism of inhibition, novel functions, and a revised nomenclature. J Biol Chem 2001; 276: 33293-33296.

[17] Lubka-Pathak M, Shah AA, Gallozzi M, Müller M, Zimmermann U, Löwenheim H, Pfister M, Knipper M, Blin N, Schimmang T. Altered expression of securin (pttg1) and serpina3n in the auditory system of hearing-impaired tff 3-deficient mice. Cell Mol Life Sci 2011; 68: 2739-2749.

[18] Sırmacı A, Erbek S, Price J, Huang M, Duman D, Cengiz FB, Bademci G, Tokgöz-Yilmaz S, Hişmi B, Ozdağ H, Oztürk B, Kulaksizoğlu S, Yildirim E, Kokotas H, Grigoriadou M, Petersen MB, Shahin H, Kanaan M, King MC, Chen ZY, Blanton SH, Liu XZ, Zuchner S, Akar N, Tekin M. A truncating mutation in serpinb6, is associated with autosomal-recessive nonsyndromic

sensorineural hearing loss. Am J Hum Genet 2010; 86: 797-804.
[19] Demura M, Hirano T. Expression analysis of the clca gene family in mouse and human with emphasis on the nervous system. BMC Dev Biol 2009; 9: 193-210.
[20] Dettenhofer M, Zhou F, Leder P. Formin 1-isoform iv deficient cells exhibit defects in cell spreading and focal adhesion formation. PLoS One 2008; 3: e2497.
[21] Malik S. Syndactyly: phenotypes, genetics and current classification. Eur J Hum Genet 2012; 20: 817-824.
[22] Bockenhauer D, Feather S, Stanescu HC, Bandulik S, Zdebik AA, Reichold M, Tobin J, Lieberer E, Sterner C, Landoure G, Arora R, Sirimanna T, Thompson D, Cross JH, van't Hoff W, Al Masri O, Tullus K, Yeung S, Anikster Y, Klootwijk E, Hubank M, Dillon MJ, Heitzmann D, Arcos-Burgos M, Knepper MA, Dobbie A, Gahl WA, Warth R, Sheridan E, Kleta R. Epilepsy, ataxia, sensorineural deafness, tubulopathy, and KCNJ10 mutations. N Engl J Med 2009; 360: 1960-1970.
[23] Reichold M, Zdebik AA, Lieberer E, Rapedius M, Schmidt K, Bandulik S, Sterner C, Tegtmeier I, Penton D, Baukrowitz T, Hulton SA, Witzgall R, Ben-Zeev B, Howie AJ, Kleta R, Bockenhauer D, Warth R. KCNJ10 gene mutations causing EAST syndrome (epilepsy, ataxia, sensorineural deafness, and tubulopathy) disrupt channel function. Proc Natl Acad Sci U S A2010; 107: 14490-14495.
[24] Hibino H, Horio Y, Inanobe A, Doi K, Ito M, Yamada M, Gotow T, Uchiyama Y, Kawamura M, Kubo T, Kurachi Y. An ATP-dependent inwardly rectifying potassium channel, KAB-2 (Kir4. 1), in cochlear stria vascularis of inner ear: its specific subcellular localization and correlation with the formation of endocochlear potential. J Neurosci 1997; 17: 4711-4721.
[25] Tasaki I, Spyropoulos CS. Stria vascularis as source of endocochlear potential. J Neurophysiol 1959; 22: 149-155.
[26] Chen J, Zhao HB. The role of an inwardly rectifying k^+, channel (kir4.1) in the inner ear and hearing loss. Neuroscience 2014; 265: 137-146.
[27] Hou L, Pavan WJ. Transcriptional and signaling regulation in neural crest stem cell-derived melanocyte development: do all roads lead to mitf?. Cell Res 2008; 18: 1163-1176.
[28] García G, Pérez A, Campos J. Kcnj10 gene mutations causing east syndrome (epilepsy, ataxia, sensorineural deafness, and tubulopathy) disrupt channel function. Proc Natl Acad Sci U S A 2010; 107: 14490-14495.

Supplementary Table 1. Primer pairs used for qPCR and PCR

Usage/Primer pairs	Gene	Location	Oligo sequence 5'-3'
Expression analysis of murine Mitf isoforms			
Mus-Mitf-A	Mitf-A		F: gcggatttcgaagtcggggagg R: ccagccataaacgtcagcgtgc
Mus-Mitf-J	Mitf-J		F: tctcgccgtgtctctgggcatc R: ccagccataaacgtcagcgtgc
Mus-Mitf-H	Mitf-H		F: gggcttgcagaacaccttaaagg R: ccagccataaacgtcagcgtgc
Mus-Mitf-M	Mitf-M		F: ggaaatgctagaatacagtcactacc R: catgcacgacgctcgagagtgc
Mus-ACTB	β-actin		F: ccccattgaacatggcattg R: acgaccagaggcatacagg
$Mitf^{mi\text{-}\Delta M/mi\text{-}\Delta M}$ mouse genotyping			
Mus-KOtyping	Mitf	Exon M	F: ggaaagggacatgcatgcgtcaac R: acacaatcatgcacacactcccca